Simulation of Thin Film All-Solid-State Lithium Ion Batteries

Makoto Fukukawa and Lizhu Tong*
Keisoku Engineering System Co., Ltd.
1-9-5 Uchikanda, Chiyoda-ku, Tokyo 101-0047, Japan, *Corresponding author: tong@kesco.co.jp

Abstract: Three-dimensional (3D) all-solid-state lithium-ion batteries molded by nano-scale thin films are attractive, because they would allow the improvement of their conductivity dramatically. In this work, we present a simulation research based on a three-dimensional model of thin film all-solid-state lithium-ion batteries using COMSOL Multiphysics@. The calculation of tertiary current density in the electrolyte and the transport of lithium species in the electrode are coupled. The concentrations of lithium ion and lithium species and the current density are obtained in charge/discharge processes. Also, the charge/discharge curves (cell voltage *vs.* time) for various charge/discharge rates are analyzed.

Keywords: 3D all-solid-state lithium-ion batteries, Nano-scale thin film, Numerical simulation.

1. Introduction

Lithium-ion batteries have been growing for tens of year as next-generation power devices. However, they have potential safety risk due to instability of their liquid electrolyte. There is great interest in developing all-solid-state lithium-ion batteries. Because of high stability of their solid electrolyte, they are ideal micro-power sources for many applications in portable electronic devices, electric vehicles and biomedical engineering [1-3].

The conductivity of the solid electrolyte is typically several orders of magnitude lower than that of liquid electrolyte of a traditional lithium-ion battery. This is the drawback of the solid electrolyte. Three-dimensional (3D) all-solid-state lithium-ion batteries molded by nano-scale thin films on micro-pillar arrays are attractive, because they would allow the improvement of their conductivity dramatically [4]. In order to make further improvement in the technology of thin film solid-state batteries on micro-pillar arrays, an in-depth understanding of the electrochemical processes involved in the batteries is necessary. However, the measurement and evaluation of these batteries are very difficult due to their complicated structure. Therefore, the numerical simulation method becomes a powerful tool to perform the investigation.

In this work, a three-dimensional (3D) model of all-solid-state lithium-ion batteries is developed based on COMSOL Multiphysics@. The tertiary current density in the electrolyte is calculated. The transport of lithium species in the positive electrode is solved in coupling with the calculation of current density. The effects of transport of lithium ions in the electrolyte and of lithium species in the positive electrode on the properties of all-solid-state lithium-ion batteries are obtained and analyzed.

2. Numerical Method

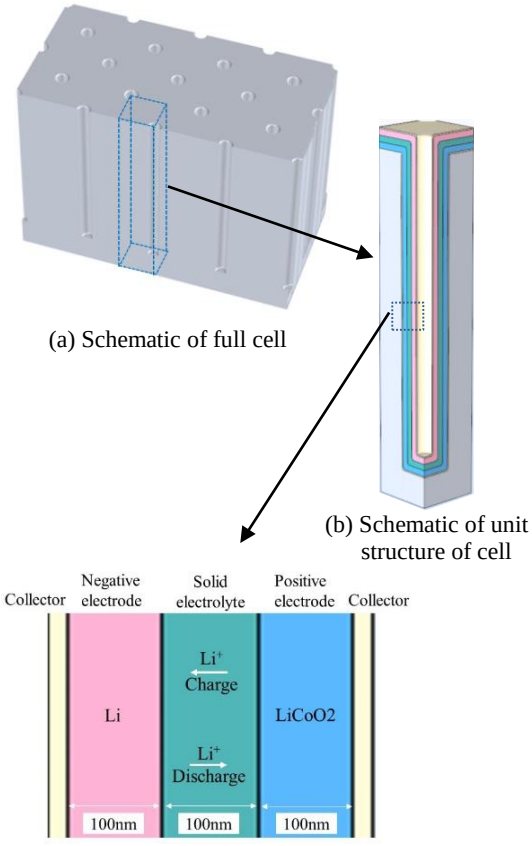

Figure 1. Schematic of 3D thin film all-solid-state lithium-ion battery.

The schematic of the all-solid-state lithium-ion battery used in this work is shown in Fig. 1, which has been described in earlier publications [5]. The full cell (Fig.1(a)) consists of an array of unit structure (Fig.1(b)), which are symmetrical to each other. It is known that the fabrication of one hundred nano-order thin film of active devices in all-solid-state lithium-ion batteries are feasible using atomic layer deposition (ALD) [5] or chemical vapor deposition (CVD) [6]. Therefore, in this work, the unit structure of cell are taken into account and the thicknesses of negative electrode, positive electrode and solid electrolyte are assigned to 100 nm. The negative electrode is metallic lithium and the positive electrode is constructed by the polycrystalline film of $LiCoO_2$. The electrolyte is a solid-state Li_3PO_4 film.

The electrochemical reactions at the negative and positive electrodes can be represented by

$$\mathrm{Li} \leftrightarrow \mathrm{Li^+} + e^- , \tag{1}$$

$$\mathrm{LiCoO_2} \leftrightarrow \mathrm{Li_{1-x}CoO_2} + x\mathrm{Li^+} + xe^-, \tag{2}$$

where the reactions shown in eqs. (1) and (2) are described using the Butler-Volmer kinetics

$$i_\mathrm{n} = Fk_\mathrm{n}\left(\frac{c_{\mathrm{Li^+}}}{c_{\mathrm{Li^+},0}}\right)^{\alpha_\mathrm{n}}\left(e^{\frac{\alpha_\mathrm{n}F\eta}{RT}} + e^{-\frac{(1-\alpha_\mathrm{n})F\eta}{RT}}\right), \tag{3}$$

$$i_\mathrm{p} = i_{0,\mathrm{p}}\left(e^{\frac{\alpha_\mathrm{p}F\eta}{RT}} + e^{-\frac{(1-\alpha_\mathrm{p})F\eta}{RT}}\right), \tag{4}$$

$$i_{0,\mathrm{p}} = Fk_\mathrm{p}\left(\frac{(c_{\mathrm{Li,max}} - c_\mathrm{Li})c_{\mathrm{Li^+}}}{(c_{\mathrm{Li,max}} - c_{\mathrm{Li,min}})c_{\mathrm{Li^+},0}}\right)^{\alpha_\mathrm{p}}\left(\frac{(c_\mathrm{Li} - c_{\mathrm{Li,min}})}{(c_{\mathrm{Li,max}} - c_{\mathrm{Li,min}})c_{\mathrm{Li^+},\mathrm{min}}}\right)^{1-\alpha_\mathrm{p}} \tag{5}$$

Here F is the Faraday's constant, k_n and k_p are the rate constants of the reactions (1) and (2), respectively, $c_{\mathrm{Li^+},0}$ is the total concentration of Li^+ in the electrolyte, α_n and α_p are the charge transfer coefficients for the reactions (1) and (2), $c_{\mathrm{Li,max}}$ and $c_{\mathrm{Li,min}}$ are the maximum and minimum levels of lithium species in the positive electrode, R is the gas constant, and T is the temperature.

In charge process, the oxidation reactions at the surface of $LiCoO_2$ occur and the produced Li^+ ions move to the negative electrode, Li, as shown in Fig. 1(c). On the contrary, for discharge process, the reduction reactions at the surface of $LiCoO_2$ occur and Li^+ ions obtained from the negative electrode come to $LiCoO_2$ and consumed at the surface of $LiCoO_2$. The chemical reaction in the electrolyte

$$\mathrm{Li^0} \leftrightarrow \mathrm{Li^+} + \mathrm{n^-} \tag{6}$$

describes the ionization reaction, where the immobile oxygen-binding lithium Li^0 is transferred to Li^+ and n^-. The transport of Li^+ and n^- is solved by the Nernst-Plank equation

$$\mathbf{N}_i = -D_i\nabla c_i + \frac{z_iF}{RT}D_i c_i \nabla\phi_l, \tag{7}$$

where c_i and D_i are the concentration and diffusion coefficient of species, respectively, z_i is the charge of species, and ϕ_l is the electrolyte potential.

The positive electrode consists of trivalent cobalt oxide species, in which the lithium ions are intercalated. Li^+ ions in $LiCoO_2$ are screened by the mobile electrons, which accompany Li^+ when they move from one interstitial site to the other. The mass transport of lithium ions inside the positive electrode can be described by the standard diffusion equation [7]. In this work, the transport of lithium species in the positive electrode is described by the Fick's law

$$\mathbf{N}_\mathrm{Li} = -D_\mathrm{Li}\nabla c_\mathrm{Li}. \tag{8}$$

where c_Li and D_Li are the concentration and diffusion coefficient of lithium species in the positive electrode, respectively.

3. Simulation results

3.1 Discharge characteristics

Figures 2-5 show the calculated results of discharge process of the all-solid-state lithium-ion battery. The battery is charged up to 4.2 V at first and then discharge starts. The discharge rates are 10, 20, 30, and 50 C. Results show that the concentration deviation from the equilibrium concentration in the electrolyte is higher for higher discharge rates. Figure 2 shows the concentration distribution of lithium in the positive electrode at 50 s for a 50 C-rate discharge. The concentration of lithium has arrived between 2.00×10^4 $\mathrm{mol/m^3}$ and 2.18×10^4 $\mathrm{mol/m^3}$. Figure 3 shows the concentration distribution of lithium ions in the electrolyte at 50 s for a 50 C-rate discharge. The maximum and minimum concentrations of lithium ions are 1.2×10^4 $\mathrm{mol/m^3}$ in the center of bottom and 8.9×10^3 $\mathrm{mol/m^3}$ around the corner of bottom as shown in Figure 3, which means that a large concentration gradient of lithium ions is formed in the bottom.

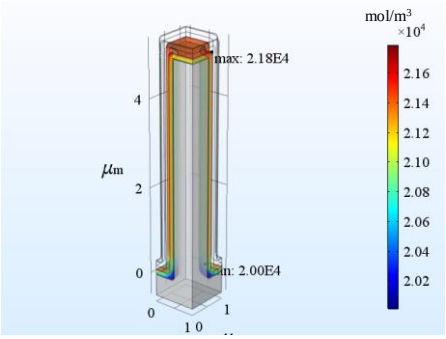

Figure 2. Concentration of lithium in the positive electrode at 50 s of discharge [mol/m^3].

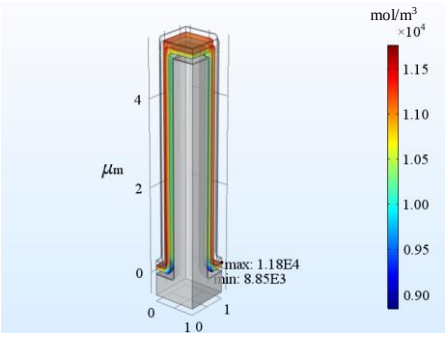

Figure 3. Concentration of lithium ions in the electrolyte at 50 s of discharge [mol/m^3]

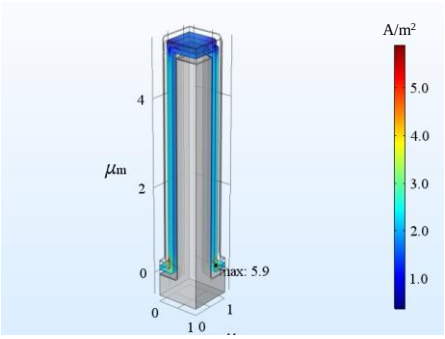

Figure 4. Current density in the electrolyte at 50 s of discharge [A/m^2].

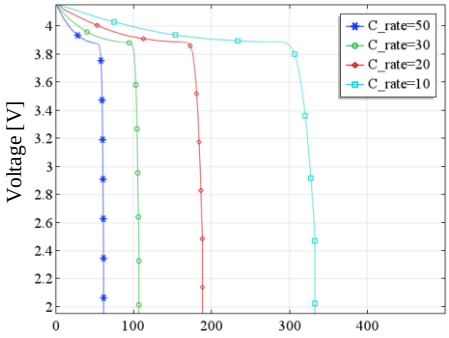

Figure 5. Discharge curves (cell voltage *vs.* time) for various discharge rates [V].

Figure 4 shows the current density in the electrolyte at 50 s for a 50 C-rate discharge. The maximum current density arrived at 5.9 A/m^2 on the corner of bottom in electrolyte. This could be a reason that causes a large concentration gradient of lithium ions in the bottom. The discharge curves for the different discharge rates are given in Fig. 5. The cell voltage before depletion is shifted downwards for higher discharge rates. This could be deduced by a fact that for higher currents, the internal losses increase.

3.2 Charge characteristics

Figures 6-9 show the calculated results of charge process of the all-solid-state lithium-ion battery. The battery is charged up to 4.2 V. The charge rates are 10, 20, 30, and 50 C. Results show that the concentration deviation from the equilibrium concentration in the electrolyte is similar to that of discharge process. Figure 6 shows the concentration distribution of lithium in the positive electrode at 50 s for a 50 C-rate charge. The concentration of lithium has arrived between 1.46×10^4 mol/m^3 and 1.58×10^4 mol/m^3, which is lower than that of discharge process because oxidation reactions occurs on the surface of positive electrode for charge process. Figure 7 shows the concentration distribution of lithium ions in the electrolyte at 50 s for a 50 C-rate charge. The maximum and minimum concentrations of lithium ions have arrived at 1.37×10^4 mol/m^3 in the center of bottom and 9.72×10^3 mol/m^3 around the corner of bottom. Figure 8 shows the current density in the electrolyte at 50 s for a 50 C-rate charge. The maximum current density arrived at 7.0 A/m^2 on the corner of bottom. The charge curves for the different charge rates are given in Fig. 9. The cell voltage by charge has a steep rise until about 3.9 V and then spreads around corresponding to the different charge rates.

As described above, the maximum current density occurs on the corner of bottom in charge/discharge processes. It is obvious that the shape of the thin film cell greatly affects performance of the battery.

4. Conclusions

This paper reports the simulation results of three-dimensional model of thin film all-solid-

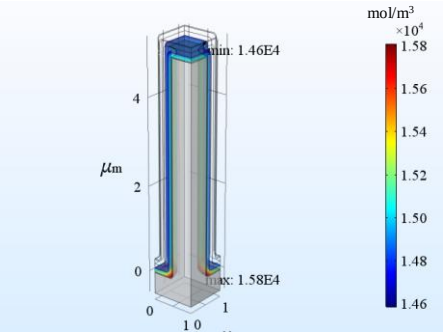

Figure 6. Concentration of lithium in the positive electrode at 50 s of charge [mol/m^3].

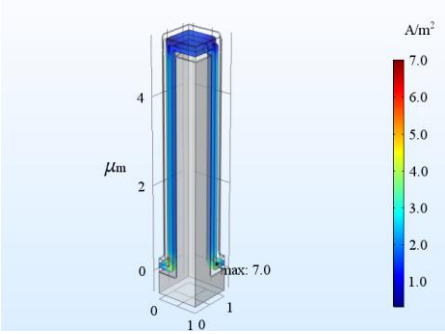

Figure 8. Current density in the electrolyte at the 50 s of charge [A/m^2].

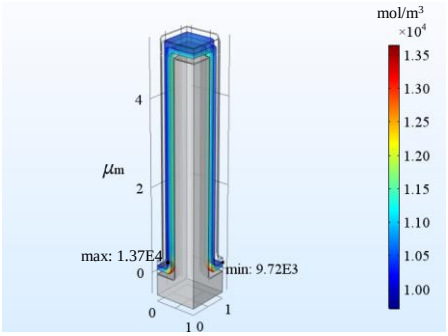

Figure 7. Concentration of lithium ions in the electrolyte at the 50 s of charge [mol/m^3].

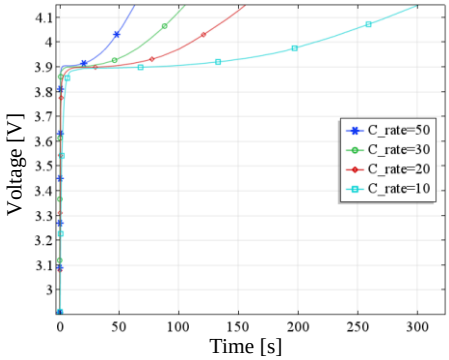

Figure 9. Charge curves (cell voltage *vs.* time) for various charge rates [V].

state lithium-ion batteries using COMSOL Multi-physics@. It is found that the battery can be quickly charged at the initial stage of charge process, and it has a smooth discharge before depletion for the different charge/ discharge rates. Also, the results shows that the maximum current density occurs on the corner of bottom in both charge/discharge processes. The present results would be beneficial to the improvement of all-solid-state lithium ion batteries molded by nano-scale thin film.

5. References

1. N. J. Dudney, "Solid-state thin-film rechargeable batteries", *Materials Science and Engineering* B **116**, 245-249 (2005).

2. A. Patil, V. Patil, D. W. Shin, J. W. Choi, D. S. Paik, and S. J. Yoon, "Issue and challenges facing rechargeable thin film lithium batteries", *Materials Research Bulletin* **43**, 1913-1942 (2008).

3. J. P. Carmo, R. P. Rocha, A. F. Silva, L. M. Goncalves, and J. H. Correia, "A thin-film rechargeable battery for integration in standalone microsystems", *Procedia Chemistry* **1**, 453-456 (2009).

4. A. A. Talin, D. Ruzmetov, and A. Kolmakov, " Fabrication, testing and simulation of all solid state three dimensional Li-ion batteries", *ACS Appl.Mater.Interfaces* **8**,(47**)**, 32385-32391(2016).

5. A. Pearse, T. Schmitt and K. E. Gregorczyk "Three-dimensional solid-state lithium-ion batteries fabricated by conformal vapor-phase chemistry", *ACS. Nano* **10**, 1021 (2018).

6. J. Xie, Jos F. M. Oudenhoven, D. Li, "High power and high capacity 3D-structured TiO_2 electrodes for lithium-ion micro batteries" *Journal of The Electrochemical Society*, **163** (10) A2385-A2389 (2016).

7. D. Danilov, R. A. H. Niessen, and P. H. L. Notten, "Modeling all-solid-state Li-ion batteries", *Journal of The Electrochemical Society* **158** (3), A215-A222 (2011).